FORUM

# Generalized Approach to Landscape-Wide Seasonal Forecasting with Temperature-Driven Simulation Models

JACQUES RÉGNIÈRE

Natural Resources Canada, Canadian Forest Service, Laurentian Forestry Centre, 1055 du P. E. P.S., P.O. Box 3800, Sainte-Fey, PQ GIV 4C7, Canada

Environ. Entomol. 25(5): 869-881 (1996)

**ABSTRACT** Determining and depicting the landscape-wide outcome of temperature-dependent ecological processes is important in the study of spatial patterns in insect ecology as well as in the efficient deployment of human and material resources for pest management. A generalized approach is proposed that consists of a temperature-driven simulation model that uses data from a limited number of strategically located points in the landscape as its input. Elevation, slope, and aspect are varied systematically for each point. Air temperature data are obtained as both real-time and climatic average data, matched with simulation points on the basis of distance, elevation, and climatic zones. Differences in latitude and elevation are compensated for with lapse rate transformations. Slope and aspect are combined into a single exposure expression, and overheating is calculated on the basis of incoming solar radiation. Landscape-wide projections of features in model output are obtained by algebraic transformation of a digital elevation model of the landscape, using a multiple regression equation relating the output feature to latitude, longitude, elevation, and exposure. The various sources of error involved in seasonal forecasting in insect ecology and management, as well as an outline of the procedure required to test the validity of landscape-wide projections, are discussed through a case study of the phenology of the spruce budworm, *Choristoneura fumiferana* (Clemens).

KEY WORDS landscape ecology, decision support, temperature-driven models, seasonality, forecasting, mapping

MANY OF THE key processes in insect ecology and pest management are temperature-dependent (Janisch 1932, Precht 1973). Temperature dependence makes the timing of events vary considerably among seasons and landscapes. Timing affects the outcome of interactions between insects, their environment, host plants, competitors, natural enemies, and humans. Short-term forecasting capabilities are needed for the efficient deployment of personnel and material resources for pest monitoring and control, particularly given the importance of reducing the environmental impact, enhancing the efficiency and reducing the costs of pest management activities (Cammell and Way 1987).

Considerable effort has been devoted to the development and testing of phenology models (Wagner et al. 1984a, b, 1991; Schaalje and van der Vaart 1988). Development of such models has been facilitated by computer algorithms (Dallwitz and Higgins 1978, Schoolfield et al. 1981, Wagner et al. 1984a) and expert systems (Logan 1988, 1989). The use of these models in ecological research and pest management is not always simple.

Computer-assisted decision support systems are tools designed to organize, integrate, and present information about a particular resource or pest management problem to a decision maker (Mumford and Norton 1984, Coulson and Saunders 1987). This information can be used to arrive at specific management prescriptions (Baskerville and Moore 1988, Power 1988, Thorpe et al. 1992).

Much of the effort in the development of decision support tools for pest management has been devoted to the creation, display, and manipulation of maps that depict the distribution and nature of resources to be protected, the associated pest populations or damage to identify areas in need of protection, and to develop optimal harvesting-protection schedules (Power and D'Eon 1992, Liebhold et al. 1993, Roberts et al. 1993). However, much less attention has focused on providing support for the development of more detailed seasonal intervention plans (Gage et al. 1982), or on studying the influence of landscape features on insect ecology (Perry 1988, Schowalter and Means 1988, Lamp and Zhao 1993, Landsberg and Gillieson 1995). Forecasting insect seasonal biology at the landscape level presents several problems, such as providing models with adequate input temperature information, carrying out large numbers of simulations, and interpreting and mapping results (Ross et al. 1989, Rock et al. 1993, Russo et al. 1993, Schaub et al. 1995).

This article proposes a generalized approach to landscape-wide forecasting of seasonal processes using temperature-driven simulation models. This approach draws many elements from the works of Russo et al. (1993) and Schaub et al. (1995) and has been incorporated into a computerized, seasonal biology forecasting system called BioSIM (Régnière et al. 1995a). Sources of error inherent to the process of seasonal biology forecasting are discussed through the analysis of a case study—the seasonal biology of spruce budworm, *Choristoneura fumiferana* (Clemens).

## Materials and Methods

**Overview.** Two methods have been used to generate landscape-wide forecasts of insect development. Russo et al. (1993) generated mesoscale temperature data from multiple regression equations that predict daily minimum and maximum air temperature from latitude, longitude, and elevation using all weather stations in an area. These data were used as input to a degree-day model of gypsy moth, *Lymantria dispar* (L.), egg hatch that was run for each pixel of a digital elevation model of the landscape, producing a map of 50% egg hatch as output. This technique uses all available regional weather data and is robust to local climatic peculiarities, but it requires considerable computational power.

Schaub et al. (1995) used weather data from a single source (base station) to run a gypsy moth development model for an array of elevations, adjusting for elevational differences from the base station through a constant vertical lapse rate (0.5°C/100 m). They then regressed the forecast target event output by the model (date of 50% 2nd-instar emergence) with elevation. They called the resulting equation a target function (or t-function) and used it to transform a digital elevation model of the area of interest into a target-event map. This approach has the advantages of simplicity and computational speed. However, it makes use of a single source of weather data with the inherent loss of information and risk of local bias. Also, vertical lapse rate was considered the sole source of temperature variation across the landscape, although their approach could be expanded to take into account other sources of geographic variation in temperature such as latitude, longitude, slope, and aspect (Rosenberg et al. 1983).

Both methods suggested the use of normals when forecasting or simulating expected development. Normals are temperature statistics (averages or extremes) calculated by days or months over standard periods of 30 yr that are updated every decade (the latest normal-generating period was 1961–1990). Thus, normals do not represent the natural daily fluctuations of air temperature. Their use as model input leads to considerable bias in simulated phenology (Régnière and Bolstad 1994) because of the nonlinear nature of insect developmental responses to temperature, the so-called Kaufmann effect (Werner 1992). Régnière and Bolstad (1994) devised a simple method to restore daily variation around normals (see also Bruhn 1980).

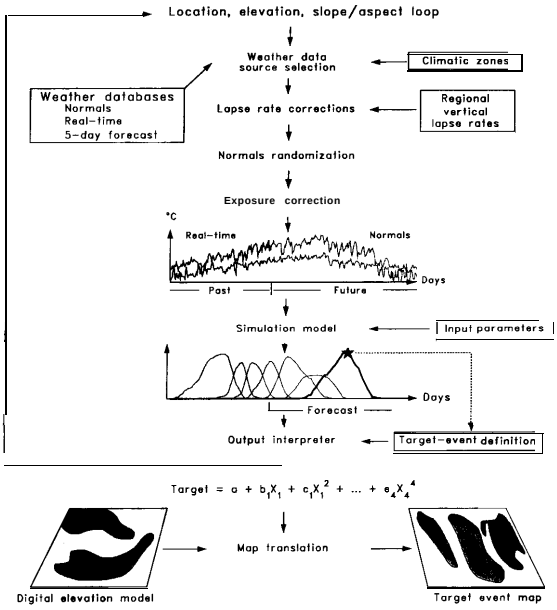


**Fig. 1.** Outline of proposed approach to landscape-wide forecasting of outcome of temperature-driven seasonal processes in insect ecology and pest management (basic design of BioSIM system). Locations can be an arbitrary list or can constitute a rectangular grid over area of interest. Weather databases, climatic zone definitions (if any), and regional vertical lapse rates are implementation-specific. Target-event definition specifies feature of interest to be extracted from model output. In this example, target event may be date at which relative frequency of 7th life stage is maximum.

The generalized approach proposed here is illustrated in Fig. 1. A simulation model is run for a number of latitude, longitude, elevation, slope, and aspect combinations. Slope and aspect are combined into a single expression-exposure to sunlight. Temperature data used as input for each simulation are assembled from various nearby sources chosen from temperature databases and are corrected for differences in latitude, elevation, and exposure between the simulation point and the data source. Model output is interpreted to extract features of interest, or target events. The term "target event" is used here to remain consistent with Schaub et al. (1995), although the current approach is by no means restricted-to timing considerations. Any feature of model output can be the object of such analysis and projection to the landscape level. A relationship between the target event and latitude, longitude, elevation, and exposure is then estimated. This relationship serves as the basis for the algebraic transformation of a digital elevation model into a target event map. The methods used to select weather stations, to

compensate for differences in elevation, latitude, and exposure, and to transform a digital elevation model into a target event map are described below.

**Temperature Regime Assembly.** An input temperature regime, defined as a series of daily minimum and maximum air temperatures, is assembled for a specified target site and period of time using data from 3 geographically referenced weather databases. The 1st, called the real-time database, contains daily minimum and maximum records from an array of recording stations. The 2nd contains mean minimum, mean maximum, extreme minimum, and extreme maximum air temperature normals by month (the normals database). The 3rd is a 5-d forecast database consisting of short-term regional weather forecasts such as are generally available from weather service agencies. Data from the real-time database are used to run simulations up to the present. Normals are used to generate future air temperatures and to fill in gaps in real-time records. Five-day forecasts are used to predict air temperature over the short term. The location of temperature data sources in each database for a given target site need not be the same. The following 4 functions are performed during temperature regime assembly for a target site (Fig. 1): (1) selection of the best sources of temperature data, (2) adjustment for latitude and elevation differences between source and target sites, (3) generation of stochastic daily minimum and maximum air temperatures from monthly normals, and (4) adjustment for exposure. In the resulting time series of daily minimum and maximum air temperatures, real-time temperature data and 5-d forecasts, when available, supersede normals.

Minimum distance is the basic criterion used to select the best sources of temperature data for a target site. However, there may be situations where the density and distribution of sources of weather data in relation to the general climatology or topography of an area justifies the use of additional criteria such as elevation. Under some circumstances, it may be preferable to select a more distant source of temperature data that is at a more similar elevation. The elevation tolerance criterion is the maximum tolerable difference in elevation between source and target sites. An elevation tolerance criterion arbitrarily set at 250 m produced satisfactory results during operational testing of BioSIM in Quebec and New Brunswick (Régnière et al. 1995b). In areas where significant climatic heterogeneities exist (other than topography) and where weather stations are sparse, it may be necessary to define climatic zone boundaries within which to restrict the search for weather data sources. For example, the proximity of a significant body of water (herein the maritime effect) can constitute the basis for a climatic zone partition, as was done in the New Brunswick test (Fig. 2). When such a partition exists and is used to select sources of weather data, the system searches within a climatic zone for the station nearest the target site.

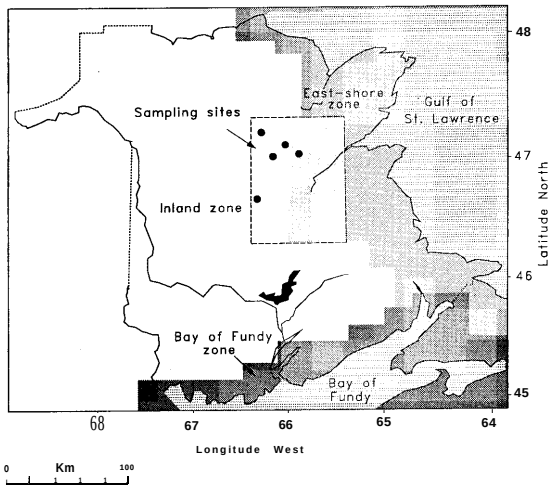


**Fig. 2.** Map of New Brunswick showing the 3 climatic zones (East Shore, Bay of Fundy, and Inland), the sampling sites, and the area boxed in covered by landscape-wide forecast generated in case study.

Once weather data sources have been selected, temperatures are adjusted for differences in elevation and latitude between the source and the target sites, using "lapse" rates. These rates vary systematically with time of year and are different for minimum and maximum air temperatures ( Régnière and Bolstad 1994). Because vertical lapse rates also vary geographically (notably as a result of maritime influences), BioSIM allows their values to be specified.

The normals database contains monthly mean and extreme minima and maxima that BioSIM uses to forecast daily temperatures by generating a stochastic series of daily values ( Régnière and Bolstad 1994). Stochastic deviations about normals are distributed normally around the mean minimum or mean maximum, with a variance that is determined from the extremes. These deviations are generated so that there is a significant correlation between daily minimum and maximum temperatures (i.e., warm and cold days). Also, minima and maxima on successive days are autocorrelated to simulate the passage of air masses (i.e., warm and cold spells). However, the algorithm does not produce significant deviations from normals as often occurs in nature. Each temperature regime thus generated is stochastically distinct, and there may be a need to replicate simulations when normals are used as model input.

Slope and aspect, through their influence on insolation, can have a significant influence on microclimate, particularly on daily maximum temperatures (Rosenberg et al. 1983). Exposure to sunlight varies with time of year, latitude, and elevation, as well as cloudiness. The system assumes that weather stations in the databases were installed on level

terrain, a standard practice in weather-monitoring equipment installation. The algorithm used in BioSIM to take slope and aspect into consideration was adapted from the model of Bolstad et al. (1996) that simulates air temperature regimes in lodgepole pine stands in mountainous terrain. This algorithm integrates radiative energy per unit surface area ($\varphi$, watts/cm$^2$) during the time of maximum irradiation (between 1100 and 1500 hours, local solar time) on a surface with specified slope and aspect. It takes into consideration the position of the sun and the amount of available solar radiation (incident and diffuse) as functions of time of day:

$$\varphi = \int_{11}^{15} I_t[\mathrm{Cos}(\Psi_t) + 0.136\ \mathrm{Cos}^2(\mathrm{Slope})]\ \mathrm{dt}, \quad (1)$$

where

$$I_t = \frac{F}{e^{\tau_t \omega_t}} \quad (2)$$

represents the proportion of total exe-atmospheric flux ($F$ = 1,373 watts/cm$^2$) that reaches the ground, $\tau_t$ is atmospheric transmittance, a function of solar zenith and site elevation, and $\omega_t$ is the length of the optical path through the atmosphere, a function of solar altitude (equation 2 from Hottel 1976, for a clear sky with 23 km visibility). In equation 1 (adapted from the solar trajectory equations of Paltridge and Platt 1976), $\Psi_t$ is the angle between the surface normal and incoming direct radiation. The value 0.136 in the 2nd term in parentheses in equation 1 is an estimate of the average proportion of incoming light that is scattered in the atmosphere and reaches a level surface as diffuse light. The amount of diffuse light irradiating a surface is a function of its slope only.

An overheating index *(v)* is computed from the difference in incident energy between the target surface ($\varphi_T$) and a level surface ($\varphi_0$), at the same elevation and latitude, relative to the largest such difference that is likely to occur during the year in the northern hemisphere, $\Delta\varphi_{max}$ = 1,500 watts/cm$^2$ over 4 h. This value was estimated iteratively with equation 1 and occurs in March at 78°N at sea level on a 45° slope with a 195° aspect. The value of *v* is thus:

$$\nu = \frac{\varphi_T - \varphi_0}{\Delta\varphi_{max}}. \quad (3)$$

This index does not exceed v = 1 and can drop as low as v = – 1.935 (in July at 64° N at sea level on a 45° slope with a 15° aspect). The extent of actual overheating of the target site also depends on cloudiness. Several authors have assumed successfully that cloudiness is correlated with the daily (unadjusted) range in temperature $R = T_x - T_n$ *(e.g.,* Régnière 1982, Bolstad et al. 1996). Thus, the daily air temperature maximum, adjusted for slope and aspect of the target site, is given by:

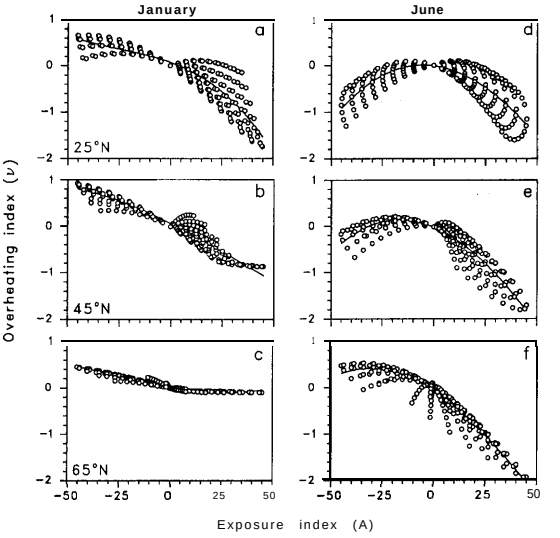


**Fig. 3.** Relationship between index of exposure *A [equation* 5) and overheating index $\nu$ (equation 3) for various combinations of slope (045°) and aspect (0–360°) at 3 latitudes (25°, 45°, and 65°N) in January (a-c) and June (d-f).

$$T''x = Tx + \nu R \Delta T_R, \quad (4)$$

where $\Delta T_R$ = 0.1429 is maximum overheating relative to a level surface, per °C of daily temperature range. This specific value of $\Delta T_R$ leads to an overheating of 4°C on a clear day with a range $R$ = 28°C on a sloped surface with v = 1.

In BioSIM, an index of northern exposure *(A,* expressed in degrees from horizontal along a north–south axis) is used to simplify simultaneous consideration of slope and aspect. This purely empirical index was designed to account for as much as possible of the variation in the overheating index *(v* in equation 4) as a function of latitude, slope, and aspect (Fig. 3):

$$A = \mathrm{Slope}.\ [\mathrm{Cos}^2(\mathrm{lat})\ .\ \phi + \mathrm{Sin}^2(\mathrm{lat})\ .\ \mathrm{Cos}(\mathrm{Aspect} - 15)], \quad (5)$$

where

$$\phi = \begin{Bmatrix} -1 & \text{if } 135 < \mathrm{Aspect} \leq 255 \\ 1 & \text{otherwise} \end{Bmatrix}. \quad (6)$$

Slope is expressed in degrees from horizontal and aspect is expressed in degrees from north. The angular shift of 15° on aspect takes into account the integration of radiant energy from 1100 to 1500 hours (equation 1) that is centered on 1300 hours (a 15° shift from solar noon).

Here, positive values of *A* are considered to be north-facing and negative values south-facing (Fig. 4). At the equator where Cos(lat) = 1 and Sin(lat) = O, all slopes oriented between 135° and 255° are considered to be south-facing (@ = – 1) and the others north-facing. At 90°N, where Cos(lat) = O and Sin(lat) = 1, only the north–south component

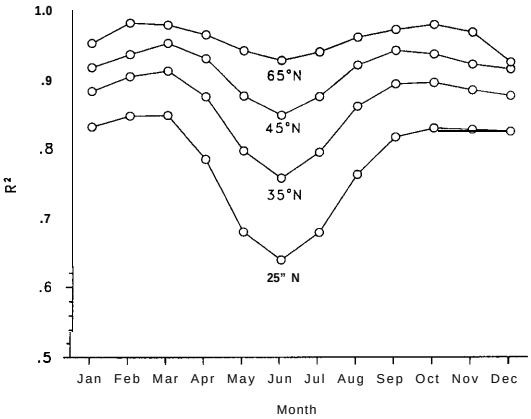


**Fig. 4.** Proportion of variation in overheating index $v$ explained by a 2nd-degree polynomial regression with exposure index $A$ at 4 latitudes (25°, 35°, 45°, and 65° N) over the year.

of slope contributes to exposure. At 45° N, both terms are equally important ($\cos^2(45) = \sin^2(45) = 0.5$).

In BioSIM, $A$ is varied from –45° to 45° for each target site and elevation. For each simulation, the average annual value of $v$ for 8 combinations of slopes and aspects that produce the specified value of $A$ is calculated and used to adjust daily maximum temperatures for exposure (using equation 4).

**Model Output Analysis and Map Generation.** The process of model output analysis and map generation is illustrated in Fig. 1. BioSIM can accommodate an arbitrary number of simulation models that are independent of the system and can be added or deleted easily from the model base (Régnière et al. 1995a). Models that are compatible with the system use time series of daily air temperature minima and maxima as input, and output daily time series of the values of state variables such as life stage frequencies, population density, parasitism rates, defoliation, etc. The system offers extensive interpretation capabilities of model output, allowing the definition of simple target events (e.g., the maximum value of a variable or the time of its occurrence) or relationships between events (e.g., difference, ratio). The event interpreter scans model output and builds an event table containing simulation point coordinates (latitude, longitude, elevation, exposure ) and event values. This table then is submitted to multiple linear regression (including polynomial terms of up to the 4th degree). The resulting regression model is then used to transform a digital elevation model into a target event map that constitutes a landscape-wide representation of model output. Slope and aspect are calculated from neighborhood elevations in the digital elevation model using the 3rd-order finite difference method (Skidmore 1989). The algorithm was designed to be used at standard USGS digital elevation models scales (i.e., 7.5' to 1° scales, with cell sizes of 30-100 m). Using it at much different scales would probably be unjustified.

The map thus created can be used directly (e.g., as suggested by Schaub et al. 1995), or in a context of broader decision support where additional sources of information such as risk and resource maps can be combined to develop pest or resource management plans.

**Case Study.** The general validity of target event forecasts is determined by the degree of realism in the air temperature data, by the precision and accuracy of the seasonal biology model used, and by the process of weather forecasting itself. This depends to a large extent on the input datasets (weather databases), the simulation model being used, and the event being forecasted. Because of this specificity, tests of such forecasting systems must be done through case studies.

The current case study is intended as an illustration of the required steps and forms the basis of a general discussion of the sources of error inherent to forecasting temperature-driven seasonal processes. It draws extensively from a test of BioSIM's performance in forecasting the phenology of the spruce budworm, *Choristoneura fumiferana* (Clemens) in New Brunswick, Canada, in 1992 and 1993 (Régnière et al. 1995b). In this test, the forecasting abilities of 2 widely different simulation models were compared—Lysyk's degree-day model (Lysyk 1989) and Régnière's process-onented model (Régnière 1982, 1983, 1984, 1987, 1990; Régnière and You 1991). Both models performed equally well, therefore results from the Régnière model only are discussed further here.

**Sources of Data.** The New Brunswick Department of Natural Resources and Energy (NBDNRE) provided the normals and real-time weather data for the province of New Brunswick (no 5-d forecast temperatures were used in this study). Also available was a definition of boundaries dividing the province into 3 climatic zones designed to take into account pronounced maritime influences near the Gulf of St. Lawrence and Bay of Fundy (Fig. 2). Data loggers were installed in 1993 in standard shelters in clearings at 5 sampling sites to record daily minimum and maximum air temperatures from early April to late July.

Spruce budworm population development was monitored every 2–3 d from May to July in 5 sites in 1992 and 1993. Sampling in 1993 was done in the immediate vicinity of the temperature recording equipment. Average instar $a$ was used as an expression of population age structure:

$$a_t = \frac{\sum_{i=2}^{8} i f_{i,t}}{\sum_{i=2}^{8} f_{i,t}}, \qquad (7)$$

where $f_i$, i = 2, 3, 4, 5, 6, 7 (pupae) and 8 (pupal cases) is the frequency of the various life stages in

foliage samples. Dates of peak life stage frequencies *(a = 3.0, 4.0, 5.0,* and *6.0)* for each sample site were estimated to the nearest day. Predicted average instar also was output by the simulation model. The model-output interpreter was used to determine the predicted date of occurrence of peak life stage frequencies based on predicted average instar.

**Temperature Regime Assembly.** Régnière et al. ( 1995b) tested the adequacy of assembled temperature regimes by comparing relationships between elevation and average air temperature from April to July for observed (on-site) and assembled temperature regimes. However, these authors did not address the issue of slope and aspect. The influence of exposure on daily maximum air temperature in regimes assembled by BioSIM was compared with observations made by Dickison and Greenbank (1972) in the same area of New Brunswick. Exposure was varied systematically from $-30^{\circ}$ to 30" northern exposure, and temperature regimes were assembled using the 5 sets of on-site weather records as a basis. Daily maximum temperatures in June were averaged over the sites, and regression analysis was used to estimate the overheating effect of exposure (in °C per 10° south). The same relationship was calculated for 13 June 1993, a typical warm, sunny day: observed maximum, 31.75°C; minimum, 11.O°C; range, 20.75°C).

**Model Bias and Precision.** Régnière et al. (1995b) tested model bias and precision. Bias was computed by averaging the deviations between observed and simulated dates of peak average instars over the 5 sites and 4 life stages *(a* = 3.0, 4.0, 5.0, and 6.0), using on-site temperature records as model input. Precision was calculated by averaging the absolute values of deviations. The same calculations were made for simulations using temperature regimes assembled from the NBDNRE databases. Bias and precision of model output using on-site and assembled temperature regimes were compared with t-tests (comparisons not made by the original authors). In addition, Régnière et al. (1995b) compared observed and predicted relationships between elevation and dates of peak larval instars using on-site temperature data.

Temperature regimes assembled by applying a range of exposures (from — 30° to 30° northern exposure) to the records of each on-site station were used as input for the Régnière model. The date at which average instar reached *a* = 4 was recorded. This value of *a* is a likely timing target for control of spruce budworm with *Bacillus thuringiensis* in New Brunswick (Carter and Lavigne 1994). Also, 2 series of simulations were conducted for 9 locations in a regular 3 x 3 grid within the area delimited by (46° 23' N, 65°30' W) and (47° 23' N, 66° 30' W) (Fig. 2). For each location, elevation and exposure were varied from O to 500 m in 100-m increments and from —45° to 45° in 15°— increments (378 simulations in each series). In the 1st series, the 1993 on-site temperature records were used as model input. In the 2nd series, only data from the NBDNRE normals database were used in temperature regime assembly. Relationships between the date of occurrence of *a = 4,* and latitude, longitude, elevation, and exposure were estimated from model output by multiple regression analysis. Using the results of the 2nd simulation series, a target event map of the expected target event (date at which *a* = 4) was obtained by algebraic transformation of a digital elevation model from the delimited area.

**Forecasting Performance.** Régnière et al. (1995b) determined the overall patterns of forecasting error associated with the 4 target larval indices *(a* = 3.0, 4.0, 5.0, and 6.0) by varying systematically the length of the forecast period. The process involved the use of a gradually increasing amount of on-site temperature data in model input which simulates the accumulation of real-time temperature data as a season progresses. The results obtained by these authors for the 1992 and 1993 seasons are illustrated in a somewhat different manner here to clarify the interaction between length of the forecast period and time into the growing season that an event is expected to occur. The changing values of forecast dates of occurrence of each peak larval index were graphed as a function of time as they converged toward the actual target events.

## Results

**Case Study.** *Temperature Regime Assembly.* Régnière et al. ( 1995b) found no differences in the slopes or intercepts of relationships between elevation and average April-July air temperatures among on-site records, temperature regimes assembled by BioSIM for these sites, or records in the NBDNRE real-time weather database. Thus, compensation for differences in elevation and latitude between source and target sites in this case study performed quite adequately.

The slope of relationships between exposure and daily maximum air temperature on 13 June, 1993 (a warm, sunny day) was 0.56°C per 10° slope along a north-south axis. This value is similar to observations made by other authors in forest canopies on sunny summer days; Dickison and Greenbank (1972) found 0.50°C per 10° slope exposure in the same area of New Brunswick; Lorenz (1969, as cited by Dickison and Greenbank 1972) measured 0.56°C per 10° slope in German forests. The effect of exposure on average daily maximum temperature over the entire month of June 1993 was somewhat less pronounced (0.38°C per 10° slope) as a result of lower average daily temperature ranges. Daily temperature range is correlated with cloudiness, which in turn reduces insolation (equation 4). The relationship between exposure and maximum air temperature was strongly nonlinear at all elevations (Fig. 5a). Dickison and Greenbank (1972) observed that canopy temperature in mid-

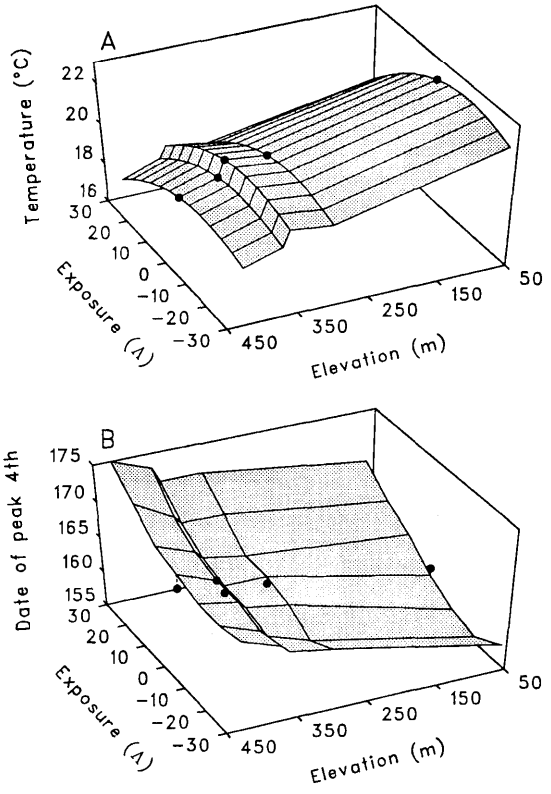


**Fig. 5.** (A) Relationship between elevation, exposure (slope and aspect), and average daily maximum air temperature among 5 sampling sites in New Brunswick in June 1993. (B) Relationship between elevation, exposure, and predicted date of occurrence of peak spruce budworm 4th instar in same sampling in 1993. Closed circles are observed values.

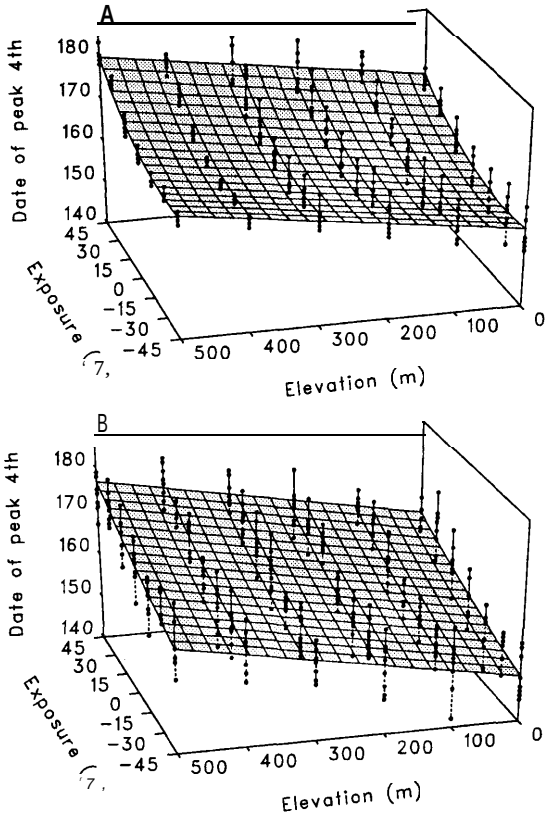


**Fig. 6.** (A) Relationship between elevation, exposure (slope and aspect), and expected date of occurrence of peak spruce budworm 4th instar in New Brunswick in 1993, based on real-time air temperature records from stations within area delimited by 46° 23' N, 65° 30' W and 47° 23' N, 66° 30' W (3 X 3 grid), (B) Same relationship based on temperature regimes generated from normals (stochastic) from normals-generating stations in same area.

summer decreased on south-facing slopes exceeding 12° in slope ( – 12° in this study). BioSIM predicted this accurately. However, the same authors suggested that temperature leveled off on north-facing slopes exceeding 20°, although their data do not show this clearly. BioSIM predicted that temperatures should decrease continually with increasing northern slope.

*Model Bias and Precision.* Régnière et al. (1995b) reported no significant bias in predicting spruce budworm development using Régnière's phenology model with either on-site (0.4 d) or assembled (-0.8 d) temperature regimes as input. This slight difference was not statistically significant ($t$ = 1.18, df = 37, $P$ > 0.25). Model precision did not differ significantly whether on-site (±2.26 d) or assembled (±2.78 d) temperature regimes were used ($t$ = –0.75, df = 35, $P$ > 0.46).

The same authors also reported that predicted and observed relationships between spruce budworm development and elevation were not significantly different. Simulation results in the current study suggest that the influence of elevation on development is somewhat more pronounced in near-level terrain than on steep slopes (Fig. 5b). A significant interaction was found between elevation and exposure ($F$ = 9.5; df = 1, 30; $P$ < 0.004) that explained only =1.4% of the total variation in predicted dates of peak 4th instar. At the lowest elevation (61 m), peak 4th instar was reached 11 d later in steep north slopes (exposure 30") than in south slopes (-20°). At the highest elevation (425 m), this difference was only 8 d. This interaction probably resulted from the nonlinear nature of the insect's developmental responses to temperature (Régnière 1982, 1987, 1990).

A significant elevation and exposure interaction was not found in the results of the multiple regression analysis of the simulation outputs for the first 3 X 3 grid-point series (Fig. 6a). The regression model used in this analysis,

$$\text{Peak}_4 = a + b \cdot \text{Lat} + c \cdot \text{Lon} + d \cdot \text{Ele} + e \cdot \text{Exp} + f \cdot \text{Exp}^2 + g \cdot \text{Ele} \cdot \text{Exp} + \epsilon, \quad (8)$$

explained 85% of the variation in the date of oc-

**Table 1. Multiple regression analysis of relationship between predicted date of occurrence of peak 4th-instar spruce budworm, latitude, longitude, elevation, and exposure (equation 8)**

| Term | *F* | df | *P* | Partial $R^2$ | Coefficient |
|---|---|---|---|---|---|
| Intercept, a | — | — | | — | 265.95 ± 24.23 |
| Latitude, b | 33.4 | 1 | <0.001 | 0.014 | 1.730 ± 0.299 |
| Longitude, c | 90.2 | 1 | <0.001 | 0.037 | –2.841 ± 0.299 |
| Elevation, d | 756.8 | 1 | <0.001 | 0.407 | 0.0197 ± 0.0007 |
| Exposure, e | 329.7 | 1 | <0.001 | 0.310 | 0.1311 ± 0.0072 |
| Exposure$^2$, f | 195.2 | 1 | <0.001 | 0.080 | 0.00219 ± 0.00016 |
| Elevation exposure, g | 0.22 | 1 | >0.637 | 0.000 | –0.00001 ± 0.00002 |
| Error | | 30 | — | 0.848[a] | |

Simulations using 1993 temperature data from the NBDNRE real-time weather database.
[a] Total $R^2$.

currence of peak 4th instar in that series (Table 1). Partial $R^2$ values indicate the relative importance of each independent variable in explaining this variation: elevation explained 40.7%, exposure (including both terms ) 39%, longitude 3.7%, and latitude 1.4%. Because there was no stochastic variation in temperature regimes used as input, the 15% unexplained variation represents "lack of fit."

The same regression model (equation 8), applied to the results of the second 3 X 3 grid-point series (based on normals), explained 72% of the variation in the target event (Table 2). Most of the extra residual variability stems from the use of stochastic–normal temperature regimes as model input (Fig. 6b). The target event map of expected dates of peak 4th-instar occurrence generated by transformation of the digital elevation model is shown in Fig, 7. The predicted influence of slope and aspect on insect development is clearly visible on this map.

*Forecasting Performance.* On average over the 1992 and 1993 sampling sites, forecast dates of peak 3rd, 4th, 5th, and 6th instar occurrence converged to within 48 h of the actual event dates (Fig. 8). Development of spruce budworm in 1992 was considerably faster than could have been expected from normals. Early-season forecasts were correspondingly late compared with actual event dates (Fig. 8a). In contrast, development in 1993 was slower than normal, and early forecasts were much earlier than actual events (Fig. 8b). Despite this difference in the direction of forecast error, the rate at which the forecasts converged toward the approaching actual events was quite similar between years. In both cases, the earliest event (peak 3rd instar) was not accurately forecast until within 4 d of its actual occurrence. The forecast date of peak 6th instar converged to a stable date at least 30 d before the actual event. Convergence of forecasts for 4th and 5th instars were intermediate (≈10 and 20 d, respectively).

## Discussion

The method used here to project the output of temperature-driven seasonal biology models to the landscape level offers several advantages over the methods proposed by Russo et al. (1993) and Schaub et al. (1995). First, it provides a direct analysis of the influence of landscape features on the ecological processes being studied rather than on the underlying temperatures as was done by Russo et al. (1993). However, contrary to the method of Schaub et al. (1995), the method used here makes use of as much weather information as may be available for a given area and explicitly takes into account several major sources of geographical variation in temperature other than elevation—slope and aspect, latitude, longitude, and regional effects such as maritime influences. Because of its ability to use weather data from several sources in the generation of a target event map, the method used here is not as sensitive to errors in data from single weather stations as that of Schaub et al. (1995). However, for implementation in areas with very sparse weather stations (such as northern Canada),

**Table 2. Multiple regression analysis of the relationship between predicted date of occurrence of peak 4th-instar spruce budworm, latitude, longitude, elevation, and exposure (equation 8)**

| Term | *F* | df | *P* | Partial $R^2$ | Coefficient |
|---|---|---|---|---|---|
| Intercept, a | | — | — | — | 112.34 ± 40.74 |
| Latitude, b | 11.9 | 1 | <0.001 | 0.009 | 1.738 ± 0.503 |
| Longitude, c | 1.29 | 1 | >0.257 | 0.001 | –0.571 ± 0.503 |
| Elevation, d | 488.9 | 1 | <0.001 | 0.370 | 0.0266 ± 0.0012 |
| Exposure, e | 154.1 | 1 | <0.001 | 0.336 | 0.1507 ± 0.0012 |
| Exposure$^2$, f | 3.22 | 1 | >0.073 | 0.002 | 0.00047 ± 0.00026 |
| Elevation . exposure, g | 0.41 | 1 | >0.523 | 0.000 | –0.00003 ± 0.00004 |
| Error | — | 30 | — | 0.718[a] | |

Simulations using temperature data from the NBDNRE normals weather database.
[a] Total $R^2$.

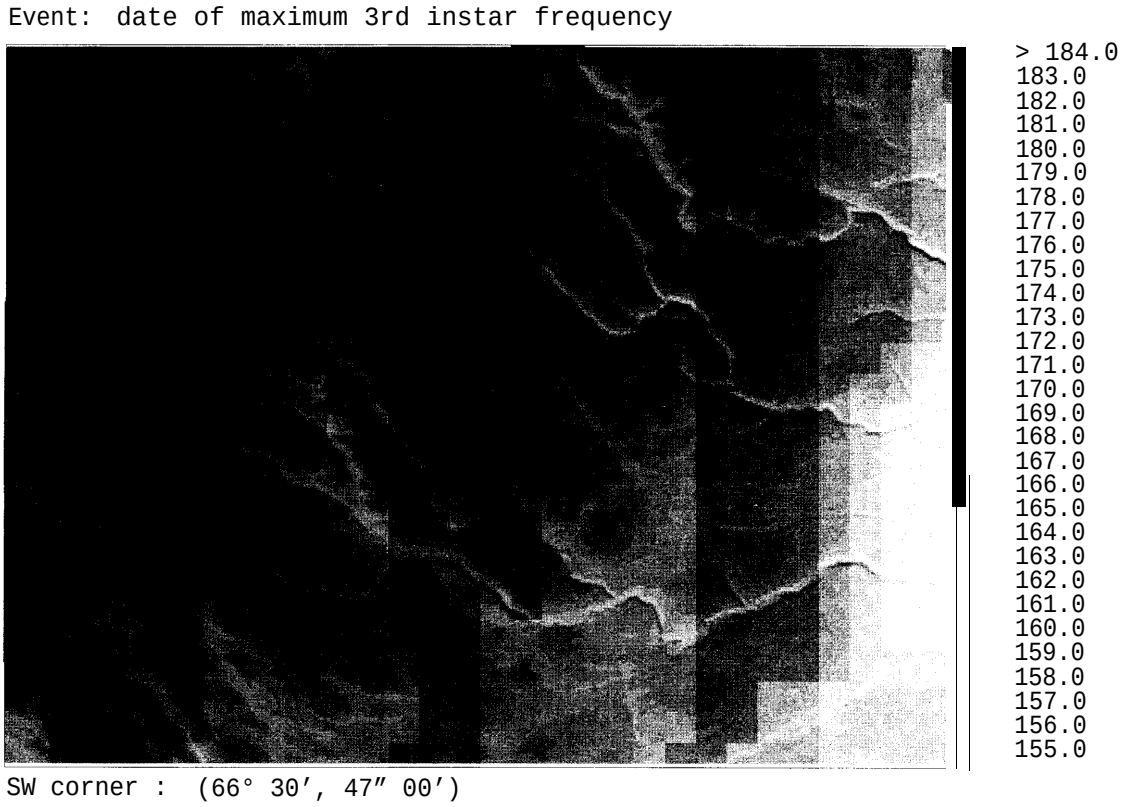


**Fig. 7.** Target event map of date of occurrence of spruce budworm peak 4th instar, calculated from a digital elevation model of area delimited by 47° O' N, 65°38' Wand 47° 8' N, 65° 30' W.

it may be necessary to generate synthetic weather data with algorithms such as those used by Russo et al. (1993). Such data could be incorporated into augmented weather databases for use in BioSIM.

Using BioSIM to generate target-event maps (sensu Schaub et al. 1995) requires less computer time than the method of Russo et al. (1993) because the analysis of model output can be based on a much smaller number of simulations. The difference in computing power requirements can be considerable. For example, generating the map shown in Fig. 7 with the method of Russo et al. (1993) would have required >130 h on a Pentium-133 computer compared with 45 min with BioSIM. This method also restores stochasticity to normals used in seasonal weather forecasting to accommodate the Kaufman effect (Werner 1992). It can also handle a large number of simulation models and can extract and analyze a wide variety of model output features. The resulting target event map can be used in ecological research as well as in pest management, directly or as an additional layer of information for decision-support tools using geographical information systems.

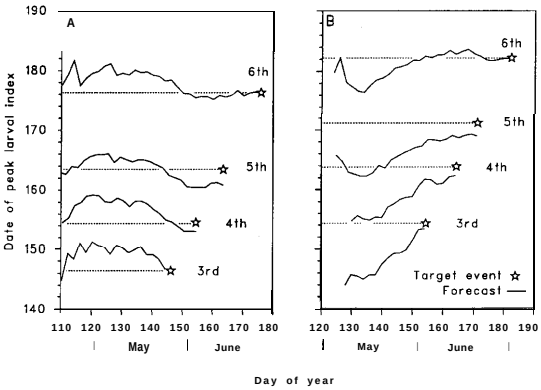


**Fig. 8.** Convergence of forecast dates with observed dates of occurrence of peak larval indices 3, 4, 5, and 6 over the season among sampling sites in New Brunswick (after Régnière et al. 1995a). (A) 1992. (B) 1993. Open stars indicate dates of actual events. Spring temperatures in 1992 were cooler than normals but were warmer in 1993.

The method used here was originally developed to deal with landscapes at a scale of 10–100 km (cell sizes of 30-100 m). However, it can be adapted for application to much larger landscapes (e.g., cells >1 km). Of course consideration of slope and aspect at such low resolution would make little sense. Two modifications implied by such an increase in scale are as follows: (1) selection of more numerous simulation points, using actual point elevations rather than varying elevation systemati-

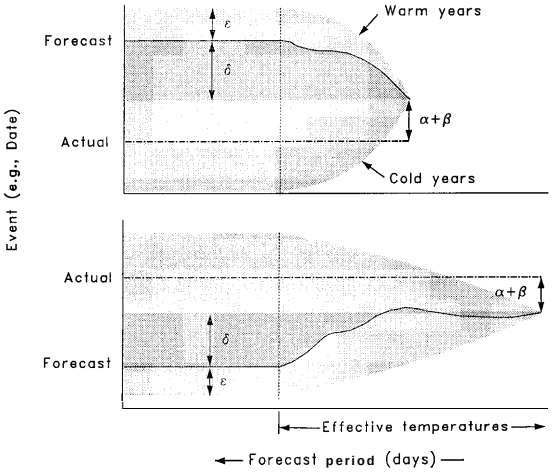


**Fig. 9.** Schematic representation of the 4 sources of error associated with forecasting of insect development and their effect on predictability of seasonal events. Sources $\alpha$ and $\beta$ are caused by model error (including microclimate and thermoregulation) and inadequate climate matching. Sources $\delta$ and l are related to forecasting process; $\in$ is random error caused by use of stochastic normals; $\delta$ is caused by systematic deviations between actual weather of a season and normals. (A) Error funnel for an early-occurring event (e.g., peak spruce budworm 3rd instar), (B) Error funnel for a late-occurring event (e.g., peak spruce budworm 6th instar).

tally for each location; and *(2)* analysis of spatial features in predicted target events using geostatistical methods such as kriging or kriging with external covariates (Liebhold et al. 1993), or multiple additive models with explicit spatial modeling (Preisler et al. 1996).

Forecasts of target events in pest management (or of the outcome of any temperature-dependent ecological processes) are only as reliable as the models used to generate them and the temperature regimes used as model input. An additional, unavoidable, and perhaps more insidious source of forecast unreliability is inaccuracy of seasonal forecasting. To discuss the issue of seasonal forecast reliability, it is useful to formally distinguish the various sources of error involved.

Assuming that measurement error associated with observed events is negligible, 4 sources of error can affect forecasts made by temperature-driven simulation models. These are illustrated in Fig. 9. The first 2, $\alpha$ and $\beta$, can cause deviations between model predictions and observed events even when the model is driven by actual on-site temperature input (no forecasting). Error source $\alpha$ represents the inaccuracy of the simulation model itself, caused by inadequate or incomplete descriptions of the processes being modeled. This error also includes differences between the temperature experienced by the organism and air temperature (microclimate, thermoregulation). It causes random (imprecision) or systematic (bias) deviations between model output and actual events. Model validation using on-site temperature data as input and comparing simulation results with observations taken in the same site can provide information on the magnitude and characteristics of $\alpha$ error. Many seasonal models (e.g., Régnière 1982) take microclimate into explicit consideration.

The 2nd source of error, $\beta$, is caused by differences between actual on-site temperature and the temperature regime used as model input. It is unusual for on-site temperature data to be available in the operational use of models. Several factors can lead to $\beta$ error: inadequate data source matching, erroneous lapse rate corrections or other landscape effects such as cold air drainage or terrain shading, and errors in the temperature records themselves. The magnitude of $\beta$ can be determined only if $\alpha$ is known.

The other 2 sources of error, $\delta$ and $\in$, apply to events for which real-time temperature data are not yet available. This implies weather forecasting, either from records of past years or from normals to which stochastic variation is restored. In either case, the fluctuations about expected (normal) temperature regimes cause corresponding uncertainty in model forecasts. The random component of this uncertainty ($\in$) can be reduced to a negligible level by replicating simulations and averaging model output. How much replication is needed depends on several factors, particularly the length of the forecast period (the amount of forecast temperature data relative to real-time data), the degree of precision required of the model's output, and the specific process being simulated. The systematic (patterned) component of forecast uncertainty ($\delta$) is the result of systematic deviation of actual temperature in any given year from normals. The resulting model predictions deviate correspondingly. Thus, in a cold year, forecast events tend to be earlier than observed, and vice versa. Such systematic deviations vanish gradually during a season as the amount of effective real-time temperature data available increases. Here, the term effective refers to those temperatures that can induce significant development, and is therefore specific to the exact temperature-dependent responses involved in the prediction. The magnitude and pattern of $\delta$ error can be known only in retrospect.

One important characteristic of the $\delta$ component of forecast error is the rate at which it converges to O, leaving only $\alpha$ and $\beta$ as error sources. This convergence rate is highly dependent on the amount of development (effective temperature) required to reach the target event. Early-occurring events require a short time series of effective temperatures, and daily stochastic deviations of temperature regimes have a large impact on the actual event. Late-occurring events, on the other hand, require a longer temperature time series and are accordingly less sensitive to daily random fluctuations that tend to "average out" by the phenomenon of regression to the mean. Thus, as a general rule, it is far easier to forecast later- than earlier-

occurring events. In our case study, the date of spruce budworm peak 3rd instar is, by nature, highly unpredictable, whereas the date of peak 6th instar can be forecast accurately almost 1 mo in advance in New Brunswick. For this reason, it may be necessary to use short-term temperature predictions to forecast early-occurring events adequately (such as spruce budworm 3rd instar). BioSIM offers this possibility through its 5-d forecast weather database.

Minimizing and estimating $\alpha$ error is an issue that is normally dealt with by model developers. BioSIM has been developed to minimize the amplitude of $\beta$ error. The vertical lapse rates used by default in the system (and in the present case study) are those estimated by Régnière and Bolstad (1994) from an array of weather stations in and around the Great Smoky Mountains in western North Carolina. Different vertical lapse rate estimates can and should be provided as input to BioSIM's temperature assembly algorithm (Fig. 1) so that the system could be used in areas distant from the eastern Atlantic portion of North America. For example, the pronounced maritime effect present in eastern New Brunswick could very well affect regional vertical lapse rates. However, the use of carefully delineated climatic zones in the weather station selection process probably accommodated this influence to a large extent.

Corrections for latitudinal temperature gradients are relatively small and should have little effect on assembled temperature regimes except in areas where weather stations are very sparse (such as in the Canadian North). In our case study, elevation, slope, and aspect accounted for most of the variation in predicted dates of peak 4th-instar spruce budworm frequency (series 1, 85%; series 2, 72%). Latitude and longitude may actually not be of much use as predictors in the transformation of digital elevation models into target event models unless the area under consideration is highly heterogeneous climatically. In such cases, particularly where weather station density is low, climatic zone definitions may be required for adequate landscape-wide forecasting of temperature-driven processes. In the case study discussed here, longitude had slightly more predictive power than latitude (3.7 versus 1.4%), probably because longitudinal climatic heterogeneity existed in the study area along the boundary of the East Shore climatic zone.

Compensation of temperature regimes for slope and aspect using the incident-light approach of Bolstad et al. (1996) produced overheating figures that compared quite well with observations in forested canopies in summer ( Dickison and Greenbank 1972). However, overheating can be far more pronounced in other types of vegetation, particularly in grasses and exposed soils (Paltridge and Platt 1976). Therefore, modifications would be required to use this algorithm in an agricultural context (particularly the value of $\Delta T_R$ in equation 4). The predicted impact of slope and aspect on insect development was not validated, however. Data for such validation in the case of spruce budworm do not exist at this time. The validity of predictions concerning the relationship between elevation and spruce budworm development ( Régnière et al. 1995b) indicates that the model simulates the insect's microclimate adequately and that the insect does not thermoregulate to an overriding extent. However, there are well-documented examples where thermoregulatory behavior overrides the influence of latitude, elevation, and perhaps slope and aspect on the temperatures experienced by the insect (see Rock et al. 1993).

## Acknowledgments

Thanks are extended to P. Bolstad for sharing his exposure algorithm, and to D. Lavigne, P. Brouillette, D. Gray, P. Bolstad, J. Logan, and 2 anonymous reviewers for their comments on the manuscript. This research was supported in part by the Spray Efficacy Research Group and the Canadian Green Plan initiative.

## References Cited

**Baskerville, G., and T. Moore. 1988.** Forest information systems that really work. For. Chron. 64: 136-140.

**Bolstad, P. V., J. A. Logan, and B. J. Bentz. 1996.** Modeling air and phloem temperatures in lodgepole pine: landscape-scale microhabitat predictions for *Dendrochtonus ponderosae*. Ecol. Model. (in press).

**Brnuhn, J. A. 1980.** A stochastic model for simulation of daily weather. Prot. Ecol. 2: 100–208.

**Cammell, M. E., and M. J. Way. 1987.** Forecasting and monitoring, pp. 1–26. *in* A. J. Bum, T. H. Coaker, and P. C. Jepson [eds. ], Integrated pest management. Academic, New York.

**Carter, N. E., and D. Lavigne. 1994.** Protection spraying against spruce budworm in New Brunswick 1993. New Brunswick Department of Natural Resource Energy, Fredericton, NB.

**Coulson, R. N., and M. C. Saunders. 1987.** Computer-assisted decision making as applied to entomology. Annu. Rev. Entomol. 32: 415-437.

**Dallwitz, M. J., and J. P. Higgins. 1978.** User's guide to DEVAR: a computer program for estimating development rate as a function of temperature. Commonwealth Scientific and Industrial Research Organisation, Division of Entomology Report 2. NSW, Australia.

**Dickison, R. B. B., and D. O. Greenbank. 1972.** The spruce budworm problem and topographic variation of forest canopy radiation temperatures, pp. 11 1–1 19. *In* D. White [cd.], proceedings the 1st Canadian Symposium on Remote Sensing. Canadian Department of Energy, Mines and Resources, Ottawa, ON, Canada.

**Gage, S. H., M. E. Whalen, and D. J. Miller. 1982.** Pest event scheduling system for biological monitoring and pest management. Environ. Entomol. 11: 1127–1133.

**Hottel, H. 1976.** A simple model for estimating the transmittance of direct solar radiation through clear atmospheres. Sol. Energy. 18: 129–134.

**Janisch, E. 1932.** The influence of temperature on the life history of insects. Trans. R. Entomol. Sot. Lend. 80: 137-168.

**Lamp, W. O., and L. Zhao. 1993.** Prediction and manipulation of movement by polyphagous, highly mobile pests. J. Agric. Entomol. 10:267-281.

**Landsberg, J., and D. S. Gillieson. 1995.** Regional and local variation in insect herbivory, vegetation and soils of eucalypt associations in contrasted landscape positions along a climatic gradient. Aust. J. Ecol. 20: 299-315.

**Liebhold, A. M., R. E. Rossi, and W. P. Kemp. 1993.** Geostatistical and geographic information systems in applied insect ecology. Annu. Rev. Entomol. 38:303-328.

**Logan, J. A. 1988.** Toward an expert system for development of pest simulation models. Environ. Entomol. 17: 359–376.

1989. Toward an expert system for pest simulation models: lessons learned from application. Br. Crop Prot. Count. Monogr. 43: 233–243.

**Lysyk, T. J. 1989.** Stochastic model of eastern spruce budworm (Lepidoptera: Tortricidae) phenology on white spruce and balsam fir. J. Econ. Entomol. 82: 1161-1168.

**Mumford, J. D., and G. A. Norton. 1984.** Economics of decision making in pest management. Annu. Rev. Entomol. 29: 157–174.

**Paltridge, G. W., and C.M.R. Platt. 1976.** Radiative processes in meteorology and climatology. Elsevier, New York.

**Perry, D. A. 1988.** Landscape pattern and forest pests. Northwest Environ. J. 4: 213–228.

**Pickering, J., W. W. Hargrove, J. D. Dutcher, and H. C. Ellis. 1990.** RAIN: a novel approach to computer-aided decision making in agriculture and forestry. Comput. Electron. Agric. 4: 275–282.

**Power, J. M. 1988.** Decision support systems for the Forest Insect and Disease Survey and for pest management. For. Chron. 64: 132–135.

**Power, J. M., and S. P. D'Eon. 1992.** Quantizing pest-caused forest depletion using geographic information. Can. For. Serv. Petawawa Natl. For. Inst. Inf. Rep. PI-X-105.

**Precht, H. 1973.** Temperature and life, rev. Springer, Berlin.

**Preisler, H. K., N. G. Rappaport, and D. L. Wood. 1996.** Regression methods for spatially correlated data: an example using beetle attacks in a seed orchard. For. Sci. (in press).

**Régnière, J. 1982.** A process-oriented model of spruce budworm phenology (Lepidoptera: Tortricidae). Can. Entomol. 114: 811–825.

**1983.** An oviposition model for the spruce budworm, *Choristoneuru fumiferrana (* Lepidoptera: Tortricidae). Can. Entomol. 115:1371-1382.

**1984.** A method of describing and using variability in development rates for the simulation of insect phenology. Can. Entomol. 116: 1367–1376.

**1987.** Temperature-dependent development of eggs and larvae of *Choristoneura fumiferana* (Clem. ) ( Lepidoptera: Tortricidae) and simulation of its seasonal history. Can. Entomol. 119:717-728.

**1990.** Diapause termination and changes in thermal responses during postdiapause development in larvae of the spruce budworm, *Choristoneura fumiferana.* J. Insect Physiol. 36: 727–735.

**Régnière, J., and P. Bolstad. 1994.** Statistical simulation of daily air temperature patterns in eastern North America to forecast seasonal events in insect pest management. Environ. Entomol. 23: 1368–1380.

**Régnière, J., and M. You. 1991.** A simulation model of spruce budworm ( Lepidoptera: Tortricidae) feeding on balsam fir and white spruce. Ecol. Model. 54: 277–297.

**Régnière, J., B. Cooke, and V. Bergeron. 1995a.** BioSIM: a computer-based decision support tool for seasonal planning of pest management activities. User's manual. Can. For. Serv. Que. Inf. Rep. LAU-X-116.

**Régnière, J., D. Lavigne, R. Dickison, and A. Staples. 1995b.** Performance analysis of BioSIM, a seasonal pest management planning tool, in New Brunswick in 1992 and 1993. Can. For. Serv. Que. Inf. Rep. LAU-X-115.

**Roberts, E. A., F. W. Ravlin, and J. S. Fleischer. 1993.** Spatial data representation for integrated pest management programs. Am. Entomol. 39: 92–107.

**Rock, G. C., R. E. Stinner, J. E. Bachelor, L. A. Hull, and H. W. Hogmire, Jr. 1993.** Predicting geographical and within-season variation in male flights of four fruit pests. Environ. Entomol. 22: 716–725.

**Rosenberg, N. J., B. L. Blad, and S. B. Verma. 1983.** Microclimate, the biological environment, 2nd ed. Wiley, New York.

**Ross, D. W., J. Pickering, J. D. Berg, and C. W. Berisford. 1989.** Mapping Nantucket pine tip moth (Lepidoptera: Tortricidae) phenology in Georgia. Linn. Entomol. Sci. 24:405415.

**Russo, J. M., A. W. Liebhold, and J.G.W. Kelley. 1993.** Mesoscale weather data as input to a gypsy moth ( Lepidoptera: Lymantriidae ) phenology model. J. Econ. Entomol. 86:838-844.

**Schaalje, G. B., and H. R. van der Vaart. 1988.** Relationships among recent models for insect population dynamics with variable rates of development. Estimation and analysis of insect populations, pp. 299–312. *In* L. McDonald, B. Manly, J. Lockwood, and J. Logan [eds.], Lecture notes in statistics 55. Springer, New York.

**Schaub, L. P., F. W. Ravlin, D. R. Gray, and J. A. Logan. 1995.** A landscape framework to predict phonological events for gypsy moth (Lepidoptera: Lymantriidae) management programs. Environ. Entomol. 24: 10–18.

**Schoolfield, R. M., P.J.H. Sharpe, and C. E. Magnuson. 1981.** Non-linear regression of biological temperature-dependent rate models based on absolute reaction rate theory. J. Theor. Biol. 88: 719–731.

**Schowalter, T. D., and J. E. Means. 1988.** Pest response to simplification of forest landscapes. Northwest Environ. J. 4: 342–343.

**Skidmore, A. K. 1989.** A comparison of techniques for calculating gradient and aspect from a gridded digital elevation model. Int. J. Geogr. Inf. Syst. 3: 323–334.

**Thorpe, K. W., R. L. Ridgway, and R. E. Webb. 1992.** A computerized data management and decision support system for gypsy moth management in suburban parks. Comput. Electron. Agric. 6: 333–345.

**Wagner, T. L., H. I. Wu, P.J.H. Sharpe, R. M. Schoolfield, and R. N. Coulson. 1984a.** Modeling insect development rates: a literature review and application of a biophysical model. Ann. Entomol. Sot. Am. 77: 208–220.

**Wagner, T. L., H. I. Wu, P.J.H. Sharpe, and R. N.** CouIson. 1984b. Modeling distributions of insect development time: a literature review and application of the Weibull function. Ann. Entomol. Sot. Am. 77: 475483.

**Wagner, T. L., R. L. Olson, and J. L. Willer. 1991.** Modeling arthropod development time. J. Agric. Entomol. 8: 251–270.

**Werner, S. P. 1992.** Performance of phonological models under variable temperature regimes: consequences of the Kaufman or rate summation effect. Environ. Entomol. 21: 659–699.

*Received for publication 6 December 1995; accepted 29 May 1996.*